# A numerical Green's function for multiple cracks in anisotropic bodies

**W. T. ANG**[1] and **J. C. F. TELLES**[2]
[1]*Division of Engineering Mechanics, School of Mechanical and Production Engineering, Nanyang Technological University, Singapore 639798*
[2]*Federal University of Rio de Janeiro, COPPE/UFRJ, Programa de Engenharia Civil, Rio de Janeiro, Brazil*

**Abstract**. The numerical construction of a Green's function for multiple interacting planar cracks in an anisotropic elastic space is considered. The numerical Green's function can be used to obtain a special boundary integral method for an important class of two-dimensional elastostatic problems involving planar cracks in an anisotropic body.

**Key words**: numerical Green's function, boundary integral method, cracks, anisotropic body.

**This is the original manuscript of the article published in**:
Journal of Engineering Mathematics 49 (2004) 197-207.

# 1 Introduction

Through the use of a suitable Green's function, an elastostatic crack problem may be formulated in terms of boundary integral equations whose path of integration does not include the crack faces. When such boundary integral equations are employed to obtain a boundary element method for the numerical solution of the crack problem, it is not necessary to model and discretize the crack faces. Furthermore, with the singular behavior of the elastic stress at the crack tips automatically built into the formulation, the numerical computation of the displacement and the stress fields near the crack tips can be accurately carried out [1]-[2].

However, the derivation of the required Green's function is a mathematically sophisticated task. The complexity involved depends on the geometry of the cracks as well as the boundary conditions imposed upon them. Ana-

lytical Green's functions seem to be available only for cracks with relatively simple geometries and boundary conditions: a single traction-free planar crack in an anisotropic space [1]-[2], a single fully closed planar crack in an anisotropic space [3], a single traction-free planar crack in an isotropic space [4], and a single traction-free arc crack in an isotropic space [5]. In general, one may find it difficult, if not impossible, to derive the required Green's function explicitly in a suitable exact form.

To apply the Green's function approach to solve a wider and a more general class of crack problems, Telles and his co-researchers proposed a numerical technique, based on the hypersingular integral formulation of crack problems, for determining the required Green's function [6]-[10] in an isotropic space. With the work in [6] as a guide, the present paper seeks to construct a numerical Green's function for arbitrarily located traction-free planar cracks in an anisotropic space under two-dimensional elastostatic deformations. The analysis presented is valid for any general anisotropic material, that is, the material is not assumed to possess any particular symmetries in its anisotropy, and it allows for a coupling of antiplane and inplane deformations. The numerical Green's function is employed to derive a boundary integral method for the numerical solution of an elastostatic crack problem involving an infinitely long anisotropic cylinder with a finite cross-section. Some specific problems are solved using the boundary integral method and the numerical results obtained are presented.

## 2 A class of crack problems

With reference to a Cartesian co-ordinate frame denoted by $0x_1x_2x_3$, consider an infinitely long anisotropic cylinder whose interior contains $P$ arbitrarily located planar cracks. The geometries of the cylinder and the cracks do not change along the $x_3$-axis. The exterior boundary of the cylinder is denoted by $C$, the region between $C$ and the cracks by $R$ and a typical $k$-th crack by $\gamma^{(k)}$. It is assumed that the cracks do not intersect with one another or the exterior boundary $C$. On the plane $x_3 = 0$, the boundary $C$ appears as a simple closed curve and the crack $\gamma^{(k)}$ as a straight cut with tips $(a^{(k)}, b^{(k)})$

and $(c^{(k)}, d^{(k)})$. For the purpose of the present paper, $\gamma^{(k)}$ is taken to be a directed straight line segment from $(a^{(k)}, b^{(k)})$ to $(c^{(k)}, d^{(k)})$.

At each and every point on the boundary $C$, either the displacements or the tractions are prescribed in such a way that the cracks open up and become traction-free. The prescribed displacements and/or tractions are assumed to be independent of the spatial co-ordinate $x_3$ and time. The problem is to determine the displacement and the stress fields throughout the body.

From a mathematical standpoint, one has to solve the equilibrium equation of elasticity given by the system of elliptic partial differential equations

$$c_{ijkp}\frac{\partial^2 u_k}{\partial x_j \partial x_p} = 0 \text{ in } R, \tag{1}$$

subject to

$$\begin{aligned} &u_i = \widetilde{u}_i \text{ for } (x_1, x_2) \in D, \quad p_i = \widetilde{p}_i \text{ for } (x_1, x_2) \in E, \\ &\sigma_{ij} m_j^{(k)} \to 0 \text{ as } (x_1, x_2) \to (y_1, y_2) \in \gamma^{(k)} \ (k = 1, 2, \cdots, P), \end{aligned} \tag{2}$$

where $u_i$ and $\sigma_{ij} = c_{ijkp}\partial u_k/\partial x_p$ are respectively the elastic displacements and stresses, $c_{ijkp}$ are the elastic moduli of the anisotropic cylinder, $p_i = \sigma_{ij} n_j$ is the traction, $n_j(x_1, x_2)$ are the components of the unit normal outward vector on $C$ at the point $(x_1, x_2)$, $D$ and $E$ are non-intersecting curves such that $D \cup E = C$, $\widetilde{u}_i$ are suitably prescribed displacements on $D$, $\widetilde{p}_i$ are the given tractions on $E$, $m_j^{(k)} = [(d^{(k)} - b^{(k)})/\ell^{(k)}, (a^{(k)} - c^{(k)})/\ell^{(k)}]$ is a unit normal vector to the crack $\gamma^{(k)}$, and $\ell^{(k)}$ is the length of $\gamma^{(k)}$, that is, $\ell^{(k)} = \sqrt{(d^{(k)} - b^{(k)})^2 + (a^{(k)} - c^{(k)})^2}$. The Einstenian convention of summing over a repeated index applies to latin subscripts running from 1 to 3.

# 3 A numerical Green's function

A function $\Phi_{ks}(x_1, x_2, \xi_1, \xi_2)$ satisfying the system of partial differential equations

$$c_{ijkp}\frac{\partial^2 \Phi_{ks}}{\partial x_j \partial x_p} = \delta_{is}\delta(x_1 - \xi_1, x_2 - \xi_2), \tag{3}$$

and the conditions on the cracks given by

$$c_{ijrp}\frac{\partial \Phi_{rs}}{\partial x_p}m_j^{(k)} \to 0 \text{ as } (x_1, x_2) \to (y_1, y_2) \in \gamma^{(k)} \ (k = 1, 2, \cdots, P), \tag{4}$$

where $\delta_{is}$ is the Kronecker-delta and $\delta$ is the Dirac-delta function, is sought.

Let $\Phi_{rs}(x_1, x_2, \xi_1, \xi_2)$ be given by

$$\Phi_{rs}(x_1, x_2, \xi_1, \xi_2) = \Phi_{rs}^{[1]}(x_1, x_2, \xi_1, \xi_2) + \Phi_{rs}^{[2]}(x_1, x_2, \xi_1, \xi_2), \tag{5}$$

$$\Phi_{rs}^{[1]}(x_1, x_2, \xi_1, \xi_2) = \frac{1}{2\pi}\,\mathrm{Re}\sum_{\alpha=1}^{3}\{A_{r\alpha}N_{\alpha j}\ln([x_1 - \xi_1] + \tau_\alpha[x_2 - \xi_2])\}\,d_{js}, \tag{6}$$

where $d_{js}$ are real constants given by

$$\mathrm{Im}\{\sum_{\alpha=1}^{3} L_{i2\alpha}N_{\alpha r}\}d_{rj} = \delta_{ij},$$

where Re and Im denote respectively the real and the imaginary part of a complex number and the constants $A_{k\alpha}$, $N_{\alpha j}$, $\tau_\alpha$, $L_{pk\alpha}$ and $N_{\alpha r}$ are related to the elastic moduli $c_{ijkp}$ and to one other as explained in references [2], [3] and [11].

The function $\Phi_{rs}^{[1]}(x_1, x_2, \xi_1, \xi_2)$ in (6) is a solution of (3). It follows that $\Phi_{rs}^{[2]}(x_1, x_2, \xi_1, \xi_2)$ is required to satisfy

$$c_{ijkp}\frac{\partial^2 \Phi_{ks}^{[2]}}{\partial x_j \partial x_p} = 0 \tag{7}$$

everywhere in the anisotropic space with the cracks $\gamma^{(1)}$, $\gamma^{(2)}$, $\cdots$, $\gamma^{(P-1)}$ and $\gamma^{(P)}$.

The conditions (4) on the cracks require that

$$c_{ijrp}\frac{\partial \Phi_{rs}^{[2]}}{\partial x_p}m_j^{(k)} \to \Lambda_{is}^{(k)}(x_1, x_2, \xi_1, \xi_2) \quad \text{as } (x_1, x_2) \to (y_1, y_2) \in \gamma^{(k)} \ (k = 1, 2, \cdots, P), \tag{8}$$

where

$$\Lambda_{is}^{(k)}(x_1,x_2,\xi_1,\xi_2) = -\frac{1}{2\pi}\,\mathrm{Re}\sum_{\alpha=1}^{3}\left\{\frac{T_{ij\alpha s}m_j^{(k)}}{[x_1-\xi_1]+\tau_\alpha[x_2-\xi_2]}\right\}, \tag{9}$$

with $T_{ij\alpha s} = L_{ij\alpha}N_{\alpha r}d_{rs}$. It is assumed that $(\xi_1,\xi_2)$ does not lie on any of the cracks.

The analysis in [12] can be used to find $\Phi_{rs}^{[2]}(x_1,x_2,\xi_1,\xi_2)$. Take

$$\Phi_{rs}^{[2]}(x_1,x_2,\xi_1,\xi_2) = \sum_{k=1}^{P}\int_{\gamma^{(k)}}\Omega_{ps}(y_1,y_2,\xi_1,\xi_2)\Lambda_{pr}^{(k)}(x_1,x_2,y_1,y_2)ds(y_1,y_2), \tag{10}$$

where $\Omega_{ps}(y_1,y_2,\xi_1,\xi_2)$ are functions yet to be determined. The system (7) is satisfied by (10).

Notice that the integration over $\gamma^{(k)}$ in (10) is one over a directed straight line segment from $(a^{(k)},b^{(k)})$ to $(c^{(k)},d^{(k)})$. As explained in the reference [12], for $(y_1,y_2)\in\gamma^{(k)}$, the function $\Omega_{rs}(y_1,y_2,\xi_1,\xi_2)$ gives the difference (jump) in the value of $\Phi_{rs}^{[2]}(x_1,x_2,\xi_1,\xi_2)$ as $(x_1,x_2)$ approaches $(y_1,y_2)$ from opposite sides of the line segment $\gamma^{(k)}$.

From (10), the conditions (8) give rise to the system of hypersingular integral equations

$$\begin{aligned}&\mathcal{H}\int_{-1}^{1}\frac{\chi_{pk}^{(q)}\Psi_{ps}^{(q)}(v,\xi_1,\xi_2)dv}{(t-v)^2} + \sum_{\substack{n=1\\ n\neq q}}^{P}\int_{-1}^{1}\Psi_{ps}^{(n)}(v,\xi_1,\xi_2)K_{pk}^{(nq)}(v,t)dv\\ &= \Lambda_{ks}^{(q)}(X_1^{(q)}(t),X_2^{(q)}(t),\xi_1,\xi_2)\ \text{for}\ -1<t<1\ (q=1,2,\cdots,P),\end{aligned} \tag{11}$$

where $\mathcal{H}$ indiactes that the integral is to be interpreted in the Hadamard finite-part sense and

$$\begin{aligned}\Psi_{ps}^{(n)}(v,\xi_1,\xi_2) &= \Omega_{ps}(X_1^{(n)}(v),X_2^{(n)}(v),\xi_1,\xi_2),\\ \chi_{pk}^{(q)} &= \frac{1}{\pi}\,\mathrm{Re}\sum_{\alpha=1}^{3}\left\{\frac{\ell^{(q)}Q_{pklr\alpha}m_l^{(q)}m_r^{(q)}}{[(c^{(q)}-a^{(q)})+\tau_\alpha(d^{(q)}-b^{(q)})]^2}\right\},\\ K_{pk}^{(nq)}(v,t) &= \frac{1}{4\pi}\,\mathrm{Re}\sum_{\alpha=1}^{3}\left\{\frac{\ell^{(n)}Q_{pklr\alpha}m_l^{(q)}m_r^{(n)}}{[\Xi^{(nq)}(v,t)+\tau_\alpha\Theta^{(nq)}(v,t)]^2}\right\},\end{aligned}$$

where $Q_{pklr\alpha} = (c_{kli1}+\tau_\alpha c_{kli2})T_{pr\alpha i}$, $\Xi^{(nq)}(v,t) = X_1^{(n)}(v)-X_1^{(q)}(t)$, $\Theta^{(nq)}(v,t) = X_2^{(n)}(v) - X_2^{(q)}(t)$, $2X_1^{(n)}(t) = [c^{(n)} + a^{(n)}] + [c^{(n)} - a^{(n)}]t$ and $2X_2^{(n)}(t) = [d^{(n)} + b^{(n)}] + [d^{(n)} - b^{(n)}]t$.

The method in the reference [13] is chosen to solve (11) numerically for $\Psi_{ps}^{(q)}(v,\xi_1,\xi_2)$. Let $\Psi_{ps}^{(n)}(v,\xi_1,\xi_2)$ be given approximately by

$$\Psi_{ps}^{(n)}(v,\xi_1,\xi_2) \simeq \sqrt{1-v^2}\sum_{j=1}^{J}\phi_{ps}^{(nj)}(\xi_1,\xi_2)U^{(j-1)}(v), \tag{12}$$

where $U^{(j)}(x) = \sin([j+1]\arccos(x))/\sin(\arccos(x))$ $(-1 < x < 1)$ is the $j$-th order Chebyshev polynomial of the second kind and $\phi_{ps}^{(nj)}(\xi_1,\xi_2)$ are parameters to be determined.

Through substituting (12) into (11) and collocating (11) by letting $t = t^{(i)} \equiv \cos([2i-1]\pi/[2J])$ for $i = 1, 2, \cdots, J$, a system of linear algebraic equations containing the unknowns $\phi_{ps}^{(ni)}(\xi_1,\xi_2)$ can be obtained as follows:

$$\begin{aligned}
&-\sum_{j=1}^{J} j\pi\phi_{ps}^{(qj)}(\xi_1,\xi_2)\chi_{pk}^{(q)}U^{(j-1)}(t^{(i)}) \\
&+\sum_{j=1}^{J}\sum_{\substack{n=1\\ n\neq q}}^{P}\phi_{ps}^{(nj)}(\xi_1,\xi_2)\int_{-1}^{1}\sqrt{1-v^2}U^{(j-1)}(v)K_{pk}^{(nq)}(v,t^{(i)})dv \\
&=\Lambda_{ks}^{(q)}(X_1^{(q)}(t^{(i)}),X_2^{(q)}(t^{(i)}),\xi_1,\xi_2) \\
&\qquad\qquad \text{for } i=1,2,\cdots,J \text{ and } q=1,2,\cdots,P.
\end{aligned} \tag{13}$$

Once $\phi_{ps}^{(ni)}(\xi_1,\xi_2)$ are determined from (13), $\Phi_{rs}^{[2]}(x_1,x_2,\xi_1,\xi_2)$ can be calculated approximately using

$$\begin{aligned}
\Phi_{rs}^{[2]}(x_1,x_2,\xi_1,\xi_2) \simeq \frac{1}{2}\sum_{n=1}^{P}\ell^{(n)}\sum_{j=1}^{J}\phi_{ps}^{(nj)}(\xi_1,\xi_2)\int_{-1}^{1}\sqrt{1-t^2} \\
\times U^{(j-1)}(t)\Lambda_{pr}^{(n)}(x_1,x_2,X_1^{(n)}(t),X_2^{(n)}(t))dt.
\end{aligned} \tag{14}$$

If the points $(x_1,x_2)$ and $(\xi_1,\xi_2)$ do not lie on any of the cracks, the numerical evaluation of $\Phi_{rs}^{[2]}(x_1,x_2,\xi_1,\xi_2)$ as given by (14) does not pose any mathematical difficulties. The definite integrals over the interval $[-1,1]$ in

(13) and (14) can be easily and accurately computed by using the numerical quadrature formula (25.4.40) listed in the mathematical handbook [14] [chapter 25, p. 889].

Notice that in (13) the coefficient of the unknown $\phi_{ps}^{(qj)}(\xi_1, \xi_2)$ is independent of the subscript $s$ and the point $(\xi_1, \xi_2)$. Thus, in solving (13) to determine $\phi_{ps}^{(qj)}(\xi_1, \xi_2)$ for different values of the subscript $s$ and for different points $(\xi_1, \xi_2)$, the square matrix containing the coefficients of the unknowns has to be computed and processed only once. For example, if the $LU$ decomposition technique together with backward substitutions is used to solve (13), one has to factorize the square matrix into a product of a lower and an upper triangular matrix only once.

Together with (13) and (14), (5)-(6) gives a useful numerical Green's function which can be employed to obtain a special boundary integral formulation for the crack problem described in Section 2. In the integral formulation, the path of integration does not include the cracks, and the evaluation of $\Phi_{rs}^{[2]}(x_1, x_2, \xi_1, \xi_2)$ at points $(x_1, x_2)$ and $(\xi_1, \xi_2)$ on the cracks is not required.

# 4 A boundary integral method

If the Green's function $\Phi_{ik}(x_1, x_2, \xi_1, \xi_2)$ satisfying (4), as given approximately by (5)-(6) together with (13) and (14), is used, a direct boundary integral formulation for the crack problem in Section 2 is given by (see [1]-[10]):

$$\lambda(\xi_1, \xi_2) u_k(\xi_1, \xi_2) = \int_C [u_i(x_1, x_2) \Gamma_{ik}(x_1, x_2, \xi_1, \xi_2) - p_i(x_1, x_2) \Phi_{ik}(x_1, x_2, \xi_1, \xi_2)] ds(x_1, x_2), \qquad (15)$$

where $\lambda(\xi_1, \xi_2) = 1$ if $(\xi_1, \xi_2)$ lies in the interior of $R$ and $\lambda(\xi_1, \xi_2) = 1/2$ if $(\xi_1, \xi_2)$ lies on a smooth part of $C$, and

$$\Gamma_{ik}(x_1, x_2, \xi_1, \xi_2) = c_{ijrs} n_j(x_1, x_2) \frac{\partial}{\partial x_s} [\Phi_{rk}(x_1, x_2, \xi_1, \xi_2)].$$

Notice that the path of integration in (15) is over only the exterior boundary $C$ of the anisotropic cylinder.

Now, from (2), either $u_i$ or $p_i$ (not both) are known at each and very point on $C$. The boundary $C$ and the integral equations (15) can be discretized to determine approximately the unknown displacements and/or tractions on $C$. To do this, the boundary $C$ is approximated using $M$ straight line segments denoted by $C^{(1)}$, $C^{(2)}$, $\cdots$, $C^{(M-1)}$ and $C^{(M)}$. Across the segment $C^{(m)}$, the displacements $u_i$ and the traction $p_i$ are approximated by constants $u_i^{(m)}$ and $p_i^{(m)}$ respectively. On a given element $C^{(m)}$, either $u_i^{(m)}$ or $p_i^{(m)}$ are known. Through approximating (15), the remaining unknown constants can be determined from the system of linear algebraic equations:

$$\begin{aligned}\frac{1}{2}u_k^{(m)} = &\sum_{n=1}^{M} u_i^{(n)} \int_{C^{(n)}} \Gamma_{ik}(x_1, x_2, \xi_1^{(m)}, \xi_2^{(m)}) ds(x_1, x_2) \\ &- \sum_{n=1}^{M} p_i^{(n)} \int_{C^{(n)}} \Phi_{ik}(x_1, x_2, \xi_1^{(m)}, \xi_2^{(m)}) ds(x_1, x_2) \\ &\qquad\qquad \text{for } m = 1, 2, \cdots, M, \end{aligned} \tag{16}$$

where $(\xi_1^{(m)}, \xi_2^{(m)})$ is the midpoint of $C^{(m)}$.

Details on the derivation of (16) and the computation of the coefficients of the linear algebraic equations may be found in the references [2] and [3].

Once $u_i^{(m)}$ and $p_i^{(m)}$ are all determined, the displacements (and hence the stresses) at any interior point $(\xi_1, \xi_2)$ in $R$ can be computed approximately using

$$\begin{aligned}u_k(\xi_1, \xi_2) = &\sum_{n=1}^{M} u_i^{(n)} \int_{C^{(n)}} \Gamma_{ik}(x_1, x_2, \xi_1, \xi_2) ds(x_1, x_2) \\ &- \sum_{n=1}^{M} p_i^{(n)} \int_{C^{(n)}} \Phi_{ik}(x_1, x_2, \xi_1, \xi_2) ds(x_1, x_2). \end{aligned} \tag{17}$$

It is also possible to determine the crack-opening displacements when $u_i^{(m)}$ and $p_i^{(m)}$ are all known. This can be done by solving the hypersingular

integral equations [6]:

$$\mathcal{H}\int_{-1}^{1}\frac{\chi_{pk}^{(q)}\Delta u_p^{(q)}(v)dv}{(t-v)^2}+\sum_{\substack{n=1\\n\neq q}}^{P}\int_{-1}^{1}\Delta u_p^{(n)}(v)K_{pk}^{(nq)}(v,t)dv=S_k^{(q)}(t)$$
$$\text{for } -1<t<1 \ (q=1,2,\cdots,P), \tag{18}$$

where $\Delta u_p^{(q)}(v)$ $(-1<v<1)$ is a function that gives the crack-opening displacements at the point $(X_1^{(q)}(v), X_2^{(q)}(v))$ of the crack $\gamma^{(q)}$, and

$$S_k^{(q)}(t)=-\sum_{n=1}^{M}u_i^{(n)}\int_{C^{(n)}}c_{kjrs}m_j^{(q)}\frac{\partial}{\partial\xi_s}[\Gamma_{ir}^{[1]}(x_1,x_2,X_1^{(q)}(t),X_2^{(q)}(t))]ds(x_1,x_2)$$
$$+\sum_{n=1}^{M}p_i^{(n)}\int_{C^{(n)}}c_{kjrs}m_j^{(q)}\frac{\partial}{\partial\xi_s}[\Phi_{ir}^{[1]}(x_1,x_2,X_1^{(q)}(t),X_2^{(q)}(t))]ds(x_1,x_2).$$

Notice that $S_k^{(q)}(t)$ is regarded as known after (16) is solved.

The system (18) can be solved numerically using the same method for (11). The unknown functions $\Delta u_p^{(n)}(v)$ are approximated using

$$\Delta u_p^{(n)}(v)\simeq\sqrt{1-v^2}\sum_{j=1}^{J}\psi_p^{(nj)}U^{(j-1)}(v), \tag{19}$$

where $\psi_p^{(nj)}$are constants determined by the system of linear algebraic equations

$$-\sum_{j=1}^{J}j\pi\psi_p^{(qj)}\chi_{pk}^{(q)}U^{(j-1)}(t^{(i)})$$
$$+\sum_{j=1}^{J}\sum_{\substack{n=1\\n\neq q}}^{P}\psi_p^{(nj)}\int_{-1}^{1}\sqrt{1-v^2}U^{(j-1)}(v)K_{pk}^{(nq)}(v,t^{(i)})dv$$
$$=\ S_k^{(q)}(t^{(i)}) \text{ for } i=1,2,\cdots,J \text{ and } q=1,2,\cdots,P, \tag{20}$$

where $t^{(i)}=\cos([2i-1]\pi/[2J])$ as in (13).

Notice that the unknown $\psi_p^{(qj)}$ in (20) has the same coefficient as $\phi_{ps}^{(qj)}(\xi_1,\xi_2)$ in (13). Thus, in solving (20) for the unknowns $\psi_p^{(qj)}$, it is not necessary to set up and process again the matrix containing the coefficients of the unknowns.

Once the unknowns $\psi_p^{(qj)}$ are determined, the crack-opening displacements can be approximately computed using (19) and crack parameters of practical interest, such as the crack energy and the relevant crack tip stress intensity factors, can also be extracted.

# 5 Numerical examples

For the purpose of applying the boundary integral approach discussed above to solve some specific crack problems, consider a particular transversely isotropic material whose elastic behavior is governed by the system

$$\begin{aligned} C\frac{\partial^2 u_1}{\partial x_1^2} + L\frac{\partial^2 u_1}{\partial x_2^2} + (F+L)\frac{\partial^2 u_2}{\partial x_1 \partial x_2} &= 0, \\ L\frac{\partial^2 u_2}{\partial x_1^2} + A\frac{\partial^2 u_2}{\partial x_2^2} + (F+L)\frac{\partial^2 u_1}{\partial x_1 \partial x_2} &= 0, \\ L\frac{\partial^2 u_3}{\partial x_1^2} + \frac{1}{2}(A-N)\frac{\partial^2 u_3}{\partial x_2^2} &= 0. \end{aligned} \tag{21}$$

For the partial differential equations (21), constants such as $A_{k\alpha}$, $L_{ij\alpha}$ and $\tau_\alpha$ which are required in the computation of the Green's function and in the boundary integral method can all be explicitly expressed in terms of the elastic constants $A$, $N$, $F$, $C$ and $L$. For further details, refer to [2] and [3].

For the first test problem, the exterior boundary of the region $R$ (on the plane $x_3 = 0$) is taken to be a square with vertices $(2, 2)$, $(-2, 2)$, $(-2, -2)$ and $(2, -2)$. The interior of $R$ contains a single crack occupying the region $-1 < x_1 < 1$, $x_2 = 0$.

A particular displacement field that satisfies (21) [or more generally (1)] in the whole of the $0x_1x_2$ plane with the single crack described above and its corresponding stress field are given by

$$u_k = \mathrm{Re}\sum_{\alpha=1}^{3} A_{k\alpha} M_{\alpha 2}(z_\alpha^2 - 1)^{1/2}, \ \sigma_{kj} = \mathrm{Re}\sum_{\alpha=1}^{3} L_{kj\alpha} M_{\alpha 2} z_\alpha (z_\alpha^2 - 1)^{-1/2}, \tag{22}$$

where $z_\alpha = x_1 + \tau_\alpha x_2$ and $[M_{\alpha k}]$ is the inverse matrix of $[L_{k2\alpha}]$. It may be verified that with (22) the conditions that the crack is traction-free are satisfied, i.e. $\sigma_{k2} = 0$ on the crack.

For a particular problem, (22) is used to generate displacements on the vertical sides of the square and tractions on the horizontal sides. The boundary integral approach together with the special numerical Green's function (as described in Sections 3 and 4) is used to solve (21) in the region $-2 < x_1 < 2$, $-2 < x_2 < 2$, which contains the traction-free crack $-1 < x_1 < 1$, $x_2 = 0$, subject to the boundary data generated by (22) on the sides of the square. If the boundary integral method really works, one should be able to recover the displacement (22) [and hence the stress as well] approximately at any interior point in the square domain through the use of (17).

For the mere purpose of illustration, the elastic constants for titanium as given by $A = 1.62$, $N = 0.92$, $F = 0.69$, $C = 1.81$ and $L = 0.467$ (in gram per centimeter per microsecond square) are chosen for computations carried out using $(M, J) = (60, 10)$ and $(M, J) = (120, 20)$.

TABLE 1. A comparison between the numerical and the exact displacement $(u_1, u_2)$ at various selected points in the interior of the square domain. The numerical results from the boundary integral method (BIM) with the numerical Green's function (NGF) obtained using $(M, J) = (60, 10)$ and $(M, J) = (120, 20)$ are given in the second and third columns respectively.

| Point $(x_1, x_2)$ | BIM with NGF $(M, J) = (60, 10)$ | BIM with NGF $(M, J) = (120, 20)$ | Exact |
|---|---|---|---|
| $(1.10, 0.00)$ | $(0.1942, 0.0000)$ | $(0.1924, 0.0000)$ | $(0.1908, 0.0000)$ |
| $(0.50, 0.80)$ | $(0.3097, 1.2149)$ | $(0.3091, 1.2169)$ | $(0.3086, 1.2188)$ |
| $(0.10, 0.70)$ | $(0.06230, 1.3775)$ | $(0.06228, 1.3796)$ | $(0.06216, 1.3816)$ |
| $(1.90, 0.10)$ | $(0.6834, 0.05311)$ | $(0.6779, 0.05202)$ | $(0.6756, 0.05190)$ |
| $(0.90, 0.20)$ | $(0.3453, 0.6529)$ | $(0.3486, 0.6551)$ | $(0.3474, 0.6558)$ |
| $(1.05, 1.05)$ | $(0.5622, 0.9116)$ | $(0.5611, 0.9134)$ | $(0.5598, 0.9148)$ |

Numerical values of the displacement $(u_1, u_2)$ computed using (17) are compared with the exact ones from (22) in Table 1 at various selected points in the interior of the square domain. (Note that $u_3 = 0$ for this particular test problem.) From the table, it is obvious that there is a good agreement between the numerical and the exact values of $(u_1, u_2)$. The numerical values improve in accuracy when the number of boundary elements $(M)$ and the number of collocation points on the crack $(J)$ used are doubled. More

specifically, if the error of the numerical displacement is calculated according to the formula

$$\text{Error } = \sqrt{(u_1^{\text{numerical}} - u_1^{\text{exact}})^2 + (u_2^{\text{numerical}} - u_2^{\text{exact}})^2},$$

then the average error of the displacement in the third column of Table 1 (given by 0.0019) is nearly two and the half times lower than that in the second column (given by 0.0045).

FIGURE 1. Plots of the numerical and the exact non-dimensionalized crack-opening displacement (COD) $\Delta u_2(x)/v_2$ for $x \in [0, 1]$.

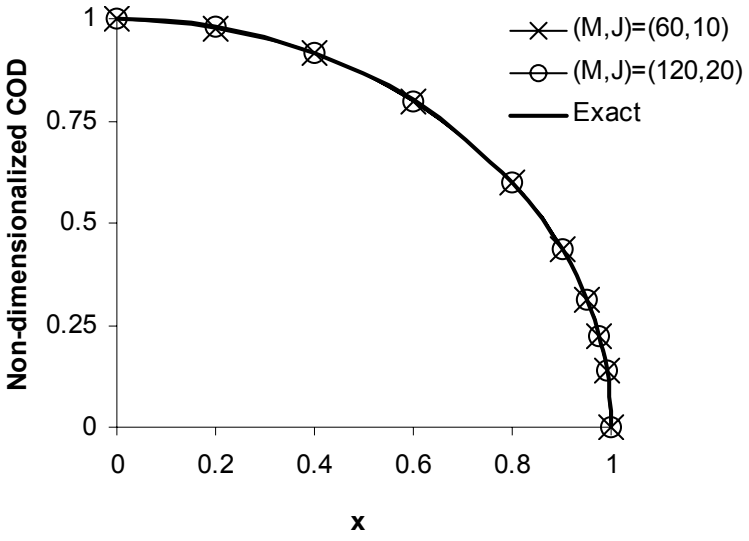


The crack-opening displacements $\Delta u_k(x_1)$ for the single crack $-1 < x_1 < 1$, $x_2 = 0$ are obtained numerically from (19) and (20). From (22), the exact crack-opening displacements are given by

$$\Delta u_k(x_1) = v_k \sqrt{1 - x_1^2}, \tag{23}$$

where $v_k = 2\,\text{Re}\{i(A_{k1}M_{12} + A_{k2}M_{22} + A_{k3}M_{32})\}$ $(i = \sqrt{-1})$. For the constants $A_{k\alpha}$ and $M_{\alpha p}$ associated with the partial differential equations (21),

it can be shown that $v_1 = 0$ and hence $\Delta u_1 = 0$. The numerically obtained crack-opening displacements indicate that $\Delta u_1(x) = 0$ and $\Delta u_2(x) = \Delta u_2(-x)$ for $-1 < x < 1$. Thus, in Figure 1, a graphical comparison between the numerical and the exact crack-opening displacements is made for only $\Delta u_2(x)/v_2$ for $x \in [0, 1]$. The numerical values of $\Delta u_2(x)/v_2$ are obtained using $(M, J) = (60, 10)$ and $(M, J) = (120, 20)$. As the numerical and the exact values of $\Delta u_2(x)/v_2$ agree to at least 2 significant figures, the three graphs in Figure 1 are visually indistinguishable.

For the crack $-1 < x_1 < 1$, $x_2 = 0$, the mode I and II stress intensity factors at the crack tips $(\pm 1, 0)$ are defined by

$$K_I^+ = \lim_{x \to 1^+} \sqrt{2(x-1)}\sigma_{22}(x, 0), \; K_I^- = \lim_{x \to -1^-} \sqrt{-2(x+1)}\sigma_{22}(x, 0)$$
$$K_{II}^+ = \lim_{x \to 1^+} \sqrt{2(x-1)}\sigma_{21}(x, 0), \; K_{II}^- = \lim_{x \to -1^-} \sqrt{-2(x+1)}\sigma_{21}(x, 0).$$

Now if the crack-opening displacements are approximately given by (19) written in the form

$$\Delta u_k(x) \simeq \sqrt{1 - x^2} \sum_{j=1}^{J} \psi_k^{(j)} U^{(j-1)}(x) \;\; \text{for} \;\; -1 < x < 1,$$

then the stress intensity factors can be shown to be approximately given by

$$K_I^{\pm} \simeq w_{p2} \sum_{j=1}^{J} \psi_p^{(j)} U^{(j-1)}(\pm 1), \; K_{II}^{\pm} \simeq w_{p1} \sum_{j=1}^{J} \psi_p^{(j)} U^{(j-1)}(\pm 1),$$

where $w_{pk} = -\operatorname{Re}\{(Q_{pk221} + Q_{pk222} + Q_{pk223})/2\}$.

TABLE 2. A comparison between the numerical stress intensity factors (SIF) from the boundary integral method with $(M, J) = (60, 10)$ and $(M, J) = (120, 20)$ and the exact values.

| SIF | BIM with NGF $(M, J) = (60, 10)$ | BIM with NGF $(M, J) = (120, 20)$ | Exact |
|---|---|---|---|
| $K_I^+ = K_I^-$ | 0.9980 | 0.9991 | 1.0000 |
| $K_{II}^+ = K_{II}^-$ | 0.0000 | 0.0000 | 0.0000 |

In Table 2, the numerical stress intensity factors obtained using $(M, J) = (60, 10)$ and $(M, J) = (120, 20)$ are compared with the exact values calculated from (22). There is a good agreement between the numerical and the exact values of the stress intensity factors.

For another specific problem governed by the system (21), take a rectangular slab occupying $-k < x_1 < k$, $-h < x_2 < h$, where $k$ and $h$ are given positive constants. The slab contains a pair of coplanar cracks $a < |x_1| < b$, $x_2 = 0$, where $a$ and $b$ are positive constants such that $a < b$. The horizontal sides of the slab are acted upon by constant antiplane shear stress $\sigma_{23} = T_0$ while the vertical sides are stress-free. For this problem, $u_1 = u_2 = 0$ and $u_3$ is governed by the third equation in (21). The reference [15] presents a semi-analytical method of solution in which the Fourier transform together with the Fourier series is applied to formulate the problem in terms of a system of hypersingular integral equations to be solved numerically.

TABLE 3. Mode III stress intensity factors at the inner and outer tips of the coplanar cracks in the rectangular slab.

| $a/\ell$ | BIM with NGF | | Reference [15] | |
|---|---|---|---|---|
| | $K_{III}^{\text{inner}}/(T_0\sqrt{\ell})$ | $K_{III}^{\text{outer}}/(T_0\sqrt{\ell})$ | $K_{III}^{\text{inner}}/(T_0\sqrt{\ell})$ | $K_{III}^{\text{outer}}/(T_0\sqrt{\ell})$ |
| 0.10 | 1.7087 | 1.3140 | 1.7112 | 1.3173 |
| 0.20 | 1.4615 | 1.2795 | 1.4649 | 1.2828 |
| 0.30 | 1.3621 | 1.2678 | 1.3654 | 1.2712 |
| 0.40 | 1.3108 | 1.2691 | 1.3140 | 1.2727 |
| 0.50 | 1.2828 | 1.2821 | 1.2861 | 1.2861 |

Here the boundary integral method together with the numerical Green's function for the two stress-free coplanar cracks is used to numerically determine $u_3$ at all points on the sides of the squares using the constants for titanium. The mode III stress intensity factors $K_{III}^{\text{inner}}$ and $K_{III}^{\text{outer}}$ at respectively the inner and the outer tips of the coplanar cracks defined by

$$K_{III}^{\text{inner}} = \lim_{x \to a^-} \sqrt{2(a-x)}\sigma_{23}(x, 0),\ K_{III}^{\text{outer}} = \lim_{x \to b^+} \sqrt{2(x-b)}\sigma_{23}(x, 0)$$

are then extracted from the boundary integral solution. In Table 3, for $k/\ell = h/\ell = 3$ and selected values of $a/\ell$, where $\ell = (b-a)/2$, the numerical

values of the non-dimensionalized stress intensity factors $K_{III}^{\text{inner}}/(T_0\sqrt{\ell})$ and $K_{III}^{\text{outer}}/(T_0\sqrt{\ell})$, obtained using $(M, J) = (96, 10)$, are compared with those given in the reference [15]. The relative discrepancy between the two sets of values for the stress intensity factors is well under 1%. When the number of boundary elements is doubled to 192, the difference is further reduced.

# 6 Final remarks

The validity of the numerical Green's function (constructed in Section 3) and the boundary integral method (described in Section 4) for the class of multiple interacting crack problems under consideration is clearly demonstrated by the numerical results obtained for the specific problems involving a particular transversely isotropic material. The numerical results also suggest that relevant crack parameters such as the crack tip stress intensity factors can be accurately extracted using the boundary integral approach presented.

It is possible to extend the numerical approach presented to include edge cracks if the method for solving the relevant hypersingular integral equations is appropriately modified as explained in [6] and [8] or as in [13]. More generally, the hypersingular integral equations for curved cracks can also be derived from equation (10) (with $\gamma^{(k)}$ being the curve giving the shape of the $k$-th crack) and solved numerically as described in [6] or [16]. A Green's function for curved cracks in anisotropic solids can then be constructed numerically.

# References


[1] M. D. Snyder and T. A. Cruse, Boundary integral analysis of cracked anisotropic plates. *International Journal of Fracture* 11 (1975) 315−328.

[2] D. L. Clements and M. D. Haselgrove, A boundary integral equation method for a class of crack problems in anisotropic elasticity. *International Journal of Computer Mathematics* 12 (1983) 267−278.

[3] W. T. Ang and D. L. Clements, A boundary integral equation method for the solution of a class of crack problems. *Journal of Elasticity* 17 (1987) 9−21.

[4] W. T. Ang, A boundary integral solution for the problem of multiple interacting cracks in an elastic material. *International Journal of Fracture* 31 (1986) 259−270.

[5] W. T. Ang, A boundary integral equation for deformations of an elastic body with an arc crack. *Quarterly of Applied Mathematics* 45 (1987) 131−139.

[6] J. C. F. Telles, G. S. Castor and S. Guimarães, A numerical Green's function approach for boundary elements applied to fracture mechanics. *International Journal for Numerical Methods in Engineering* 38 (1995) 3259−3274.

[7] L. P. S. Barra and J. C. F. Telles, A hypersingular numerical Green's function generation for BEM applied to dynamic SIF problems. *Engineering Analysis with Boundary Elements* 23 (1999) 77−87.

[8] G. S. Castor and J. C. F. Telles, The 3-D BEM implementation of a numerical Green's function for fracture mechanics applications. *International Journal for Numerical Methods in Engineering* 48 (2000) 1191−1214.

[9] J. C. F. Telles and S. Guimarães, Green's function: a numerical generation for fracture mechanics problems via boundary elements. *Computer Methods in Applied Mechanics and Engineering* 188 (2000) 847−858.

[10] S. Guimarães and J. C. F. Telles, General application of numerical Green's functions for SIF computations with boundary elements. *Computer Modeling in Engineering and Sciences* 1 (2000) 131−139.

[11] A. N. Stroh, Dislocations and cracks in anisotropic elasticity. *Philosophical Magazine* 3 (1958) 625−646.

[12] W. T. Ang and Y. S. Park, Hypersingular integral equations for arbitrarily located planar cracks in an anisotropic elastic bimaterial. *Engineering Analysis with Boundary Elements* 20 (1997) 135−143.

[13] A. C. Kaya and F. Erdogan, On the solution of integral equations with strongly singular kernels. *Quarterly of Applied Mathematics* 45 (1987) 105−122.

[14] M. Abramowitz and I. A. Stegun, *Handbook of Mathematical Functions.* New York: Dover; 1971; 1046 pp.

[15] W. T. Ang and G. P. Noone, Coplanar cracks in a finite rectangular anisotropic elastic slab under antiplane shear stresses: a hypersingular integral formulation. *Engineering Fracture Mechanics* 45 (1993) 431−437.

[16] Y. Z. Chen, A numerical solution technique of hypersingular integral equation for curved cracks. *Communications in Numerical Methods in Engineering* 19 (2003) 645−655.